



**HAL**  
open science

## Robust Mismatched Filter for Off-Grid Target

Olivier Rabaste, Jonathan Bosse

► **To cite this version:**

Olivier Rabaste, Jonathan Bosse. Robust Mismatched Filter for Off-Grid Target. IEEE Signal Processing Letters, 2019, 26 (8), pp.1147-1151. <10.1109/LSP.2019.2923054>. <hal-02298676>

**HAL Id: hal-02298676**

**<https://hal.science/hal-02298676v1>**

Submitted on 27 Sep 2019

HAL is a multi-disciplinary open access archive for the deposit and dissemination of scientific research documents, whether they are published or not. The documents may come from teaching and research institutions in France or abroad, or from public or private research centers.

L'archive ouverte pluridisciplinaire HAL, est destinée au dépôt et à la diffusion de documents scientifiques de niveau recherche, publiés ou non, émanant des établissements d'enseignement et de recherche français ou étrangers, des laboratoires publics ou privés.



HAL Authorization

# Robust Mismatched Filter for Off-Grid Target

Olivier Rabaste, *Member, IEEE*, and Jonathan Bosse

**Abstract**—In this letter, we consider the robustness of the mismatched filter in presence of off-grid target. Since for an off-grid target, the received sampled signal differs from the on-grid signal, the mismatched filter as optimized in the literature is not optimal anymore, and in particular may present a deteriorated sidelobe level. We propose here a general optimization program enabling to get an optimal mismatched filter - with respect to the Integrated Sidelobe Level (ISL) - within the resolution cell. We detail then the resulting solution in two particular radar cases, namely a Doppler steering vector and a linear chirp signal. In both cases, the proposed solution involves the Discrete Prolate Spheroidal Sequences. Simulation results show that this solution indeed provides the best ISL in the resolution cell.

**Index Terms**—Mismatched filter, Off-grid target, ISL

## I. INTRODUCTION

THE matched filter is both the filter that maximizes the Signal-to-Noise Ratio for a target buried in Gaussian noise, and the Generalized Likelihood Ratio Test solution to the detection problem involving a single target with unknown amplitude and Gaussian noise [1]. In radar applications, it consists in correlating the received signal with different copies of the transmitted waveform, these copies differing from one another by the value of a given target parameter that may be for instance delay, Doppler shift or beam angle. However this matched filter often presents high sidelobes that may prevent weak target detection in the presence of strong targets or clutter. A possible solution to this sidelobe problem consists in replacing the matched filter by a different filter providing lower sidelobes, at the expense of some loss in processing gain, and possibly in some cases a wider mainlobe [2], [3].

This mismatched filter approach has been extensively studied in the literature [2], [4], [5]. When considering a sampled waveform corresponding to a given target parameter, it has been shown that the problem of optimizing the mismatched filter with respect to the PSLR (Peak-to-Sidelobe Level Ratio) or the ISL (Integrated Sidelobe Level) objectives can be cast as a convex optimization problem under convex constraints [6]–[9], so that an optimal solution can be retrieved using interior point methods [10]. This solution is however optimal only for the corresponding sampled waveform. As soon as the target backscattered sampled waveform differs from the considered signal vector, the optimized mismatched filter is not optimal anymore and may on the contrary present higher distorted sidelobes. This problem may arise as soon as the target parameter does not belong to the sampled parameter grid, which is generally provided by the parameter resolution: for instance, in radar applications, for delay processing, waveforms are generally sampled at a sampling rate of the order of the inverse of the transmitted bandwidth; for Doppler

processing, the Doppler frequency shift is sampled at the inverse of the integration time. This is known as the off-grid target mismatch [11], [12].

Classic radar waveforms continuously depend on the delay parameter. This is the case of the extensively used “chirp” signal: sampling this chirp signal for two different delays within the same resolution cell indeed leads to two different sampled vectors. As for the Doppler shift, physical laws provide a steering vector with linear phase that continuously changes within the Doppler resolution cell. Off-grid target parameters may thus lead to deteriorated sidelobes, as well as extended targets composed of several unresolved reflectors or diffuse clutter. This problem should thus been taken into account when designing a mismatched filter. However, to our knowledge, it has never been addressed in the literature, except for a first attempt by the authors in [13] where the considered mismatched filter optimization program was set as a min-max optimization program on the sidelobe levels observed on a given set of off-grid hypotheses within the resolution cell, and the proposed - simple - solution was to reformulate this optimization program by adding additional constraints corresponding to these sampled values.

In the present article, we consider the more general problem of an ISL-based mismatched filter optimization that is robust to any off-grid mismatch or spread target/clutter within the resolution cell, in the sense that any given off-grid point-like target contribution will provide low ISL whatever its location within the cell. After a brief general mathematical presentation of the problem at hand and the proposed general solution based on a point-like target model, we will derive the corresponding optimal solution for two different waveforms, first classic phase steering vector considered in several applications (spectral analysis, Doppler radar analysis) and second, chirp signals. Interestingly, we show that the optimal solution involves in both cases well-known Discrete Prolate Spheroidal Sequences (DPSS) vectors [14] already encountered in many applications [15]–[19] and in particular in radar applications when dealing with off-grid/unresolved radar targets [11], [12].

This paper is organized as follows. In section II is presented the proposed general optimization program for robust mismatched filter. Then in section III, we focus on the derivation of the objective function in two particular cases. Finally in section IV are provided some simulation results.

## II. MISMATCHED FILTER

### A. Classic optimal filter computation

Let us consider a general radar setting where the transmitted signal is backscattered by the target with an unknown param-

eter  $\theta$  (for instance a delay, a Doppler shift or a beam angle). This signal can be represented by the  $N \times 1$  vector

$$\mathbf{s}(\theta) = [s_1(\theta), s_2(\theta), \dots, s_N(\theta)]^T,$$

where  $\cdot^T$  denotes the matrix transpose, and where  $N$  may correspond to the number of time samples, pulses or antennas, according to the considered parameter.

Let us first assume that the target is located at the center  $\theta_0$  of one resolution cell. The optimal mismatched filter for processing such a signal vector should provide the best possible correlation output, i.e. maximum energy for the signal vector  $\mathbf{s}(\theta_0)$  - namely the filter mainlobe -, while minimum output for other hypotheses - namely the filter sidelobes. The different hypotheses considered represent a grid in the parameter space. They are generally sampled at the resolution size  $\Delta$  to limit computational cost and memory size, and also to preserve orthogonality of the filter outputs. Stacking all these different hypotheses into a single matrix  $\mathbf{\Lambda}(\theta_0)$ , the output of a mismatched filter  $\mathbf{q}$  of length  $K$  can be written:

$$\mathbf{y}(\theta_0) = \mathbf{\Lambda}(\theta_0)\mathbf{q}, \quad (1)$$

where

$$\mathbf{\Lambda}(\theta_0) = \begin{bmatrix} \mathbf{s}^H(\theta_0 - Q_l\Delta) \\ \vdots \\ \mathbf{s}^H(\theta_0 - \Delta) \\ \mathbf{s}^H(\theta_0) \\ \mathbf{s}^H(\theta_0 + \Delta) \\ \vdots \\ \mathbf{s}^H(\theta_0 + Q_r\Delta) \end{bmatrix}$$

is of size  $Q \times K$  where  $K$  is the length of the mismatched filter  $\mathbf{q}$  and  $Q = Q_l + Q_r + 1$  depends on the parameter involved, since the structure of matrix  $\mathbf{\Lambda}(\theta_0)$  differs according to the parameter. Note that replacing  $\mathbf{q}$  in (1) by  $\mathbf{s}(\theta)$  provides the output of the filter matched to signal  $\mathbf{s}(\theta)$ .

The optimal filter for the ISL criteria can be obtained by solving the following constrained optimization problem:

$$\begin{aligned} \min_{\mathbf{q}} \quad & \|\mathbf{F}\mathbf{y}(\theta_0)\|_2^2 && (\text{Obj}) \\ \text{s.t.} \quad & \mathbf{s}^H(\theta_0)\mathbf{q} = \mathbf{s}^H(\theta_0)\mathbf{s}(\theta_0), && (C_E) \\ & \mathbf{q}^H\mathbf{q} \leq \alpha \mathbf{s}^H(\theta_0)\mathbf{s}(\theta_0), && (C_{LPG}) \end{aligned} \quad (2)$$

where  $\mathbf{F}$  is a diagonal matrix containing ones on the diagonal except for zero values at entries corresponding to the mainlobe [5], [9]. The objective (Obj) represents the integrated energy of the sidelobes of  $\mathbf{y}(\theta_0)$ , the first constraint ( $C_E$ ) enables to discard the trivial all-zero solution, and the second constraint ( $C_{LPG}$ ) enables to ensure that the Loss-in-Processing-Gain (LPG) is at most equal to  $-10 \log_{10} \alpha$  dB [9].

When the second constraint is discarded, the optimal solution is expressed analytically as [5]

$$\mathbf{q}_{\text{ISL}} = \frac{(\mathbf{s}^H(\theta_0)\mathbf{s}(\theta_0)) (\mathbf{\Lambda}^H(\theta_0)\mathbf{F}\mathbf{\Lambda}(\theta_0))^{-1} \mathbf{s}(\theta_0)}{\mathbf{s}^H(\theta_0) (\mathbf{\Lambda}^H(\theta_0)\mathbf{F}\mathbf{\Lambda}(\theta_0))^{-1} \mathbf{s}(\theta_0)}. \quad (3)$$

On the contrary, no analytical solution exists when the second constraint is considered, but the program is convex and can be solved efficiently by a classic convex solver, such as CVX, a MATLAB package for specifying and solving convex programs [20].

## B. Robust ISL optimal filter within the resolution cell

Solution to the optimization problem (2) provides the optimal ISL when the received signal is exactly  $\mathbf{s}(\theta_0)$ . However, in practice, parameter  $\theta$  is not known, and thus the mismatched filter computed for specific value  $\theta_0$  is not optimal anymore for any other value in the set  $\Theta_{\text{cell}} = [\theta_0 - \Delta/2, \theta_0 + \Delta/2]$ . The difference between signals  $\mathbf{s}(\theta_0)$  and  $\mathbf{s}(\theta)$  may be sufficiently important to observe a dramatic deterioration of the sidelobe level. The aim of this article is thus to develop a mismatched filter that minimizes the overall sidelobe energy within the resolution cell. This corresponds to finding the filter that minimizes the ISL for a target or clutter uniformly extended in the resolution cell, or that minimizes the mean ISL for a point off-grid target with unknown parameter  $\theta$  uniformly distributed in the resolution cell.

In order to obtain a filter robust on the resolution cell, the proposed optimization program is:

$$\begin{aligned} \min_{\mathbf{q}} \quad & \mathbb{E}_{\theta} [\|\mathbf{F}\mathbf{y}(\theta)\|_2^2] \\ \text{s.t.} \quad & \mathbf{s}^H(\theta_0)\mathbf{q} = \mathbf{s}^H(\theta_0)\mathbf{s}(\theta_0), \\ & \mathbf{q}^H\mathbf{q} \leq \alpha \mathbf{s}^H(\theta_0)\mathbf{s}(\theta_0), \end{aligned} \quad (4)$$

where the two constraints enable to discard the trivial solution and to limit the LPG provided by the filter for parameter value  $\theta_0$ . We consider here that  $\theta$  is uniformly distributed over  $\Theta_{\text{cell}}$ , reflecting the lack of prior information on  $\theta$ . Exploiting this assumption and the linearity of the expectation provides:

$$\mathbb{E}_{\theta} [\|\mathbf{F}\mathbf{y}(\theta)\|_2^2] \propto \int_{\Theta_{\text{cell}}} \|\mathbf{F}\mathbf{y}(\theta)\|_2^2 d\theta = \mathbf{q}^H \mathbf{M}_{\Theta_{\text{cell}}} \mathbf{q},$$

with  $\mathbf{M}_{\Theta_{\text{cell}}} = \int_{\Theta_{\text{cell}}} \mathbf{\Lambda}^H(\theta)\mathbf{F}\mathbf{\Lambda}(\theta) d\theta$ . Assuming that matrix  $\mathbf{M}_{\Theta_{\text{cell}}}$  is hermitian and positive definite, it can be expressed by means of its square root  $\mathbf{M}_{\Theta_{\text{cell}}}^{1/2}$  so that  $\mathbf{M}_{\Theta_{\text{cell}}} = (\mathbf{M}_{\Theta_{\text{cell}}}^{1/2})^H \mathbf{M}_{\Theta_{\text{cell}}}^{1/2}$ . In that case, the objective of the optimization program (4) is convex and can be written

$$\mathbb{E}_{\theta} [\|\mathbf{F}\mathbf{y}(\theta)\|_2^2] = \|\mathbf{M}_{\Theta_{\text{cell}}}^{1/2} \mathbf{q}\|_2^2,$$

so that (4) can be solved efficiently, either analytically if only the first constraint is considered, in which case the solution is provided by (3) where  $\mathbf{\Lambda}^H(\theta_0)\mathbf{F}\mathbf{\Lambda}(\theta_0)$  is replaced by  $\mathbf{M}_{\Theta_{\text{cell}}}$ , or by means of a convex solver if the LPG constraint is also considered. Thus the optimal mismatched filter can be obtained as soon as matrix  $\mathbf{M}_{\Theta_{\text{cell}}}$  is known, and the solution complexity is similar to the classic on-grid mismatched filter.

## III. COMPUTATION OF $\mathbf{M}_{\Theta_{\text{cell}}}$

We detail here the computation of  $\mathbf{M}_{\Theta_{\text{cell}}}$  in two cases.

### A. Steering vector for spectral or Doppler analysis

We first consider the common pure phase steering vector case encountered in several applications (spectral analysis, Doppler radar analysis from pulse trains, phase arrays, ...). In such a setting, assuming the considered vector is of length  $N_p$ , the resolution is given by  $\Delta = 1/N_p$ , and the steering vector provided by a Doppler shift  $\theta$  is expressed as:

$$\mathbf{s}(\theta) = [1, e^{j2\pi\theta}, \dots, e^{j2\pi\theta(N_p-1)}]^T. \quad (5)$$

In such a setting, all possible steering vectors are defined by parameter  $\theta \in [0, 1]$ . Sampling the parameter  $\theta$  at period  $\Delta$ , it follows that only  $N_p$  steering vectors should be considered, belonging to the grid  $\mathcal{G} = \{0, \Delta, 2\Delta, \dots, (N_p - 1)\Delta\}$ . Then, for a given off-grid shift  $\delta\theta$  defined in interval  $[-\Delta/2, \Delta/2]$ , the  $n^{\text{th}}$  row  $\mathbf{\Lambda}_n(\delta\theta)$  of  $N_p \times N_p$  matrix  $\mathbf{\Lambda}(\delta\theta)$  is:

$$\begin{aligned}\mathbf{\Lambda}_n(\delta\theta) &= \left[1, e^{-j2\pi(n\Delta + \delta\theta)}, \dots, e^{-j2\pi(N_p - 1)(n\Delta + \delta\theta)}\right] \\ &= \mathbf{s}^H(n\Delta + \delta\theta).\end{aligned}$$

Straightforward calculation enables to show that the  $(k, n)$  entry  $\mathbf{M}_{k,n}(\delta\theta)$  of matrix  $\mathbf{M}(\delta\theta) = \mathbf{\Lambda}^H(\delta\theta)\mathbf{F}\mathbf{\Lambda}(\delta\theta)$  then writes

$$\mathbf{M}_{k,n}(\delta\theta) = \mathbf{M}_{k,n}(0)e^{j2\pi(k-n)\delta\theta},$$

where matrix  $\mathbf{M}(0) = \mathbf{\Lambda}^H(0)\mathbf{F}\mathbf{\Lambda}(0)$ . Then it directly comes that matrix  $\mathbf{M}_{\Theta_{cell}}$  is equal to

$$\mathbf{M}_{\Theta_{cell}} = \mathbf{M}(0) \odot \mathbf{P}(N_p), \quad (6)$$

where notation  $\odot$  stands for the component-wise multiplication while the  $(k, n)$  entry  $\mathbf{P}_{k,n}(x)$  of matrix  $\mathbf{P}(x)$  is

$$\mathbf{P}_{k,n}(x) = \int_{-\frac{\Delta}{2}}^{\frac{\Delta}{2}} e^{j2\pi(k-n)\delta\theta} d\delta\theta = \frac{1}{x} \text{sinc}\left(\frac{k-n}{x}\right). \quad (7)$$

Interestingly, this matrix is well known in signal processing because its eigenvectors correspond to the Discrete Prolate Spheroidal Sequences (DPSS) vectors [14].

Note that a consequence of (6) is that, when  $\mathbf{q}$  is computed for a given  $\theta_0$ , then the solution  $\mathbf{q}'$  of (4) when the constraints are defined for  $\theta'_0 \neq \theta_0$  is given by  $\mathbf{q}' = \mathbf{q} \odot \mathbf{s}(\theta'_0 - \theta_0)$ .

### B. Chirp signal

Let us now consider the case of a delayed chirp signal, that can be described as the (centered) baseband continuous signal

$$c(t) = e^{j\pi\frac{B}{T_p}t^2 - j\pi Bt} \Pi_{T_p}(t),$$

where  $B$  is the chirp bandwidth,  $T_p$  the pulse duration and  $\Pi_{T_p}(t)$  the application equal to 1 if  $t \in ]0, T_p[$  and 0 otherwise. In that case, the parameter of interest is the delay, and it is possible to chose a mismatched filter of length  $K$  longer than the number of signal samples  $N$ . Considering that the received signal is sampled at the sampling period  $\Delta = 1/B$ , the correlation matrix to consider for a given off-grid delay  $\delta\theta$  defined in the interval  $[-\Delta/2, \Delta/2]$  is then of size  $(K + N - 1) \times K$  and can be expressed as

$$\mathbf{\Lambda}^*(\delta\theta) = \begin{bmatrix} c(t_N^{\delta\theta}) & 0 & \dots & \dots & \dots & \dots & 0 \\ \vdots & c(t_N^{\delta\theta}) & \ddots & & & & \vdots \\ c(t_2^{\delta\theta}) & & \ddots & 0 & & & \vdots \\ c(t_1^{\delta\theta}) & c(t_2^{\delta\theta}) & \dots & c(t_N^{\delta\theta}) & 0 & \dots & 0 \\ 0 & c(t_1^{\delta\theta}) & \ddots & \vdots & c(t_N^{\delta\theta}) & \ddots & \vdots \\ \vdots & \ddots & \ddots & c(t_2^{\delta\theta}) & & \ddots & 0 \\ 0 & \dots & 0 & c(t_1^{\delta\theta}) & c(t_2^{\delta\theta}) & & c(t_N^{\delta\theta}) \\ \vdots & & & 0 & c(t_1^{\delta\theta}) & \ddots & \vdots \\ \vdots & & & & \ddots & \ddots & c(t_2^{\delta\theta}) \\ 0 & \dots & \dots & \dots & \dots & 0 & c(t_1^{\delta\theta}) \end{bmatrix}$$

where  $t_n^{\delta\theta} = \Delta/2 + n\Delta - \delta\theta$  corresponding to the time of the  $n^{\text{th}}$  sample and we have chosen here, for simplicity of computation but without lack of generality, that for  $\delta\theta = 0$ , samples are taken at time samples  $t = \{\Delta/2, 2\Delta/2, \dots, N\Delta/2\}$ . Entries of  $\mathbf{\Lambda}^*(\delta\theta)$  are complex conjugates entries of  $\mathbf{\Lambda}(\delta\theta)$ .

Calculating matrix  $\mathbf{M}(\delta\theta) = \mathbf{\Lambda}^H(\delta\theta)\mathbf{F}\mathbf{\Lambda}(\delta\theta)$  leads to the fact that its  $(k, n)$  entry  $\mathbf{M}_{k,n}(\delta\theta)$  is given by

$$\mathbf{M}_{k,n}(\delta\theta) = \mathbf{M}_{k,n}(0)e^{j2\pi(k-n)\delta\theta/T_p},$$

where again  $\mathbf{M}(0) = \mathbf{\Lambda}^H(0)\mathbf{F}\mathbf{\Lambda}(0)$ . Thus it follows that

$$\mathbf{M}_{\Theta_{cell}} = \mathbf{M}(0) \odot T_p \mathbf{P}(BT_p), \quad (8)$$

where the  $(k, n)$  entry of matrix  $\mathbf{P}(\Theta_{cell})$  is defined in (7). Again matrix  $\mathbf{M}_{\Theta_{cell}}$  can be expressed by means of the DPSS vectors.

## IV. SIMULATION RESULTS

In this section, we will present simulation results in order to compare the performance of the proposed filter with existing solutions from the literature. We compare the proposed off-grid robust mismatched filter, denoted ‘‘OG-RMMF’’, with the classic matched filter (‘‘MF’’), the Hamming window (‘‘Hamming’’) and the mismatched filter proposed by the authors in [13] that deals with the off-grid problem in a suboptimal manner by adding off-grid constraints. This last filter, denoted ‘‘OG-MMF  $L_2$ ’’, is computed here for 5 off-grid constraints uniformly spread on  $\Theta_{cell}$ . Both mismatched filters are computed with a constraint on the LPG equal to the LPG provided by the Hamming window (provided in Table I).

We first consider the case of steering vectors for spectral analysis. The processing filter  $\mathbf{q}$  (that can be any of the previously considered filters) is computed for a given on-grid  $\theta_0$ . We present in Figure 1 its response when the received sampled signal is of the form  $\mathbf{s}(\theta_0 + \delta\theta)$  where  $\theta_0$  belongs to the grid, i.e.  $\theta_0 \in \mathcal{G} = \{0, \Delta, 2\Delta, \dots, (N_p - 1)\Delta\}$  and where the target may be either ‘‘on-grid’’ (case  $\delta\theta = 0$ ) or ‘‘off-grid’’ (target located near the edge of the resolution cell, case  $\delta\theta = 0.45\Delta$ ). The output of filter  $\mathbf{q}$  for such a target is provided by the different inner products  $\|\mathbf{s}^H(\theta + \delta\theta)\mathbf{q}\|^2$  where parameter  $\theta$  takes all possible values in the grid  $\mathcal{G}$ .

Note here that since the grid  $\mathcal{G}$  is sampled at the resolution cell, in the case of the matched filter, the different vectors  $\mathbf{s}(\theta)$  correspond to the Fourier basis and are thus perfectly orthogonal to  $\mathbf{s}(\theta_0)$ , except for  $\theta = \theta_0$ . As a well-known result, we thus observe a delta Dirac in  $\delta\theta = 0$  for the MF in Figure 1. This perfect peak is strongly degraded in the case  $\delta\theta = 0.45$ . It appears on that figure that the two mismatched filters considered provide nearly similar performance, with the proposed ‘‘OG-RMMF’’ filter being slightly better because it is optimized on the whole resolution cell while the ‘‘OG MMF  $L_2$ ’’ is optimized only on a finite discrete set of off-grid locations. Overall these two filters provide better sidelobe level than the Hamming window except in the on-grid case.

Considering the ISL itself, we compute by numerical simulation (on a thin grid) the mean ISL over the whole resolution cell, which is provided by

$$\mathbb{E}_{\theta} [ISL] = \int_{\Theta_{cell}} \|\mathbf{F}\mathbf{y}(\theta)\|_2^2 d\theta.$$

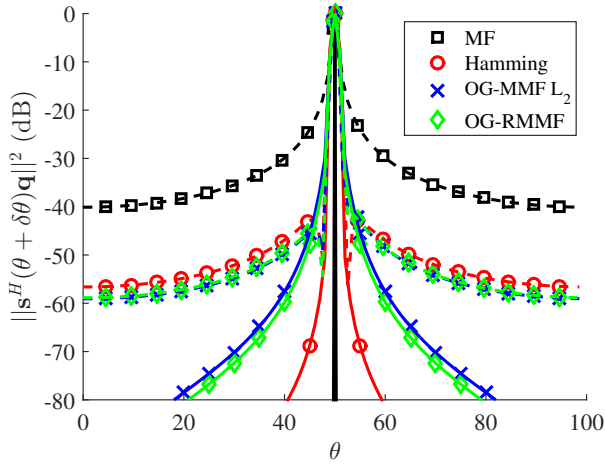


Fig. 1. Output  $\|s^H(\theta + \delta\theta)\mathbf{q}\|^2$  for different filters  $\mathbf{q}$  (matched or mismatched) versus  $\theta \in \mathcal{G} = \{0, \Delta, 2\Delta, \dots, (N_p - 1)\Delta\}$ . The target is located in cell  $\theta_0 = 50$ , and is either “on-grid” (case  $\delta\theta = 0$ , represented in straight line ‘-’) or “off-grid” (case  $\delta\theta = 0.45\Delta$ , represented in dashed line ‘- -’).  $N_p = 100$ . Case of a steering vector for spectral or radar Doppler analysis.

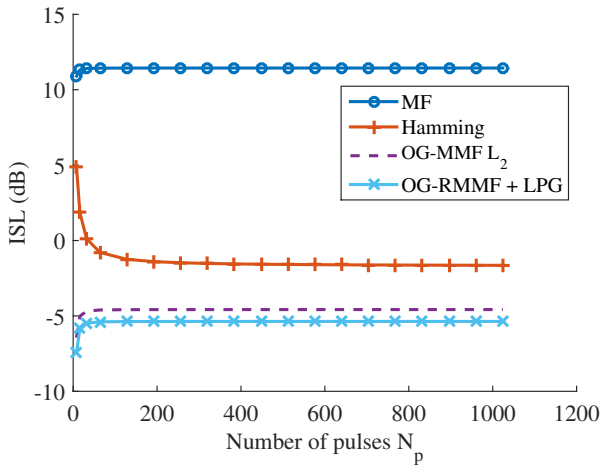


Fig. 2. ISL performance versus  $N_p$  for different reception filters. Case of a steering vector for spectral or radar Doppler analysis.

Results presented in Figure 2 that represents the ISL evolution with respect to the number of pulses  $N_p$ , corroborates the previous observations, i.e. the proposed robust mismatched filter outperforms classic filters such as the matched filter or the Hamming window filter. Note that the mismatched filter performance is obtained for a mainlobe slightly smaller than the one of the Hamming window, and for an LPG slightly smaller also: the LPG is equal to 1.35 for the Hamming window and is equal to 1.10 dB for the “OG-RMMF” filter; thus interestingly here, also the LPG is constrained to be equal to the LPG of the Hamming window, the optimal solution provides still a smaller LPG.

A similar comparison study is performed in the case of a chirp signal. In that case, the length of the mismatched filter can be chosen to be greater than the length of the signal, and thus we set it here to  $K = 3N$ . In addition

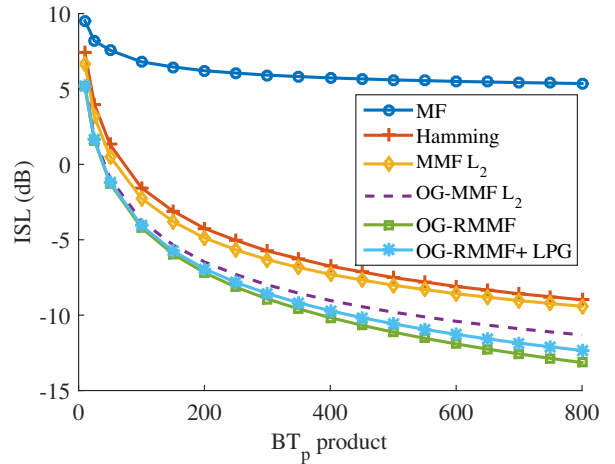


Fig. 3. ISL performance versus  $BT_p$  product for different reception filters. Pulse duration:  $T_p = 50 \mu\text{s}$ . Chirp signal case.

$BT_p$	50	100	200	500	800
Hamming	1.282	1.313	1.329	1.338	1.341
MMF $L_2$	1.282	1.313	1.329	1.338	1.341
OG-MMF $L_2$	1.282	1.313	1.329	1.338	1.341
OG-RMMF	1.649	1.764	1.863	1.968	2.008
OG-RMMF + LPG	1.281	1.313	1.329	1.335	1.340

TABLE I  
LPG (IN dB) VERSUS  $BT_p$  PRODUCT FOR DIFFERENT RECEPTION FILTERS. PULSE DURATION:  $T_p = 50 \mu\text{s}$ . CHIRP SIGNAL CASE.

to the same filters considered for the Doppler case, we also consider here the classic mismatched filter optimized for the “on-grid” signal (denoted as “MMF  $L_2$ ”) [9], and the proposed robust mismatched filter is either computed without the LPG constraint (“OG-RMMF”) or with the LPG constraint (“OG-RMMF + LPG”). We present in Figure 3 the evolution of the ISL with respect to the  $BT_p$  product, for a fixed pulse duration  $T_p = 50 \mu\text{s}$ , and the evolution of the LPG in Table I. The best filter with respect to the ISL performance is the “OG-RMMF” without LPG constraint, but it also provides the strongest LPG. The “OG-RMMF + LPG” filter provides very close ISL performance with a perfectly controlled LPG. In particular its performance is much better than the Hamming window one, for the same LPG and a slightly smaller mainlobe width. Thus the proposed method indeed enables to provide a more robust filter over the resolution cell.

## V. CONCLUSION

In this article, we have proposed an optimization program that enables to obtain a mismatched filter robust to off-grid target mismatch. The resulting objective function, defined for optimizing the ISL, has been detailed for two particular cases, a Doppler steering vector and a linear chirp. Interestingly, in both cases, the robust mismatched filter involves the DPSS vectors. Note that we used here for simplicity a grid sampled at the resolution cell. However even for an oversampled grid, the mismatch problem may occur, and the proposed solution may be computed for the corresponding grid.

## REFERENCES

- [1] S. Kay, *Fundamentals of Statistical Signal Processing. Detection theory*. Prentice Hall, 1998.
- [2] N. Levanon and E. Mozeson, *Radar signals*. Wiley, 2004.
- [3] S. Blunt and E. Mokole, "Overview of radar waveform diversity," *IEEE Aerospace and Electronic Systems Magazine*, vol. 31, pp. 2–42, 2016.
- [4] J. Baden and M. Cohen, "Optimal peak sidelobe filters for biphasic pulse compression," in *Proceedings of the IEEE International radar conference*, 1990, pp. 249–252.
- [5] K. Griep, J. Ritcey, and J. Burlingame, "Poly-Phase Codes and Optimal Filters for Multiple User Ranging," *IEEE Trans. Aerospace and Electronic Systems*, vol. 31, no. 2, pp. 752–767, 1995.
- [6] H. Lebrete and S. Boyd, "Antenna Array Pattern Synthesis via Convex Optimization," *IEEE Trans. on Signal Processing*, vol. 45, no. 3, pp. 526–532, 1997.
- [7] P. Stoica, J. Li, and M. Wue, "Transmit codes and receive filters for radar," *IEEE Signal Processing Mag.*, vol. 25, no. 6, pp. 94–109, 2008.
- [8] A. De Maio, Y. Huang, M. Piezzo, S. Zhang, and A. Farina, "Design of radar receive filters optimized according to  $l_p$ -norm based criteria," *Signal Processing, IEEE Transactions on*, vol. 59, no. 8, pp. 4023–4029, 2011.
- [9] O. Rabaste and L. Savy, "Mismatched filter optimization for radar applications using quadratically constrained quadratic programs," *IEEE Transactions on Aerospace and Electronic Systems*, vol. 51, no. 4, pp. 3107–3122, 2015.
- [10] S. Boyd and L. Vandenberghe, *Convex Optimization*. Cambridge: Cambridge University Press, 2004.
- [11] J. Bosse and O. Rabaste, "Subspace Rejection for Matching Pursuit in the Presence of Unresolved Targets," *IEEE Transactions on Signal Processing*, vol. 66, pp. 1997–2010, 2018.
- [12] O. Rabaste, J. Bosse, and J.-P. Ovarlez, "Off-grid target detection with normalized matched subspace filter," in *2016 European Signal Processing Conference (EUSIPCO)*, 2016.
- [13] O. Rabaste, J. Bosse, and L. Savy, "Approximated optimal mismatched filter for off-grid-delayed sampled continuous-phase modulations," in *2017 International Conference on Radar*, 2017.
- [14] D. Slepian, "Prolate spheroidal wave functions fourier analysis and uncertainty - V: The discrete case," *Bell Syst. Tech. J.*, vol. 57, pp. 1371–1430, 1978.
- [15] P. Forster and G. Vezzosi, "Application of spheroidal sequences to array processing," in *Proceedings of the IEEE Int. Conf. Acoust. Speech Signal Process.*, vol. 12, 1987, pp. 2268–2271.
- [16] C. Chen and P. Vaidyanathan, "MIMO Radar space-time adaptive processing using prolate spheroidal wave functions," *IEEE Trans. on Signal Processing*, vol. 56, no. 2, pp. 623–635, 2008.
- [17] M. A. Davenport and M. B. Wakin, "Compressive sensing of analog signals using discrete prolate spheroidal sequences," *Applied and Computational Harmonic Analysis*, vol. 33, no. 3, pp. 438–472, 2012.
- [18] F. Ahmad, J. Qian, and M. Amin, "Wall clutter mitigation using discrete prolate spheroidal sequences for sparse reconstruction of indoor stationary scenes," *IEEE Trans. Geosci. Remote Sens.*, vol. 53, no. 3, pp. 1549–1557, 2015.
- [19] Z. Zhu and M. Wakin, "Approximating sampled sinusoids and multiband signals using multiband modulated DPSS dictionaries," *J. Fourier Anal. Appl.*, vol. 23, pp. 1263–1310, 2017.
- [20] CVX Research, Inc., "CVX: Matlab software for disciplined convex programming, version 2.0 beta," <http://cvxr.com/cvx>, Sep. 2012.